IEEE Access
Multidisciplinary | Rapid Review | Open Access Journal

Date of publication xxxx 00, 0000, date of current version xxxx 00, 0000.

Digital Object Identifier 10.1109/ACCESS.2022.Doi Number

Adaptive Motion Control for An Autonomous Mobile Robot Based on Space Risk Map

Bin Zhang[1], Member, IEEE, Ryuji Sengoku[1], and Hun-ok Lim[1], Member, IEEE
[1]Department of Mechanical Engineering, Kanagawa University, Yokohama, Kanagawa 2218686 Japan
Corresponding author: Bin Zhang (e-mail: zhangbin@kanagawa-u.ac.jp).

ABSTRACT To make mobile robot move considerately, an adaptive motion control method integrated potential field method is proposed. Risk map is firstly defined to show the magnitude of risks in the empty spaces around objects, then the considerate path is generated based on based on risk map. The robot is controlled by using integrated potential field method. The robot can automatically move with a considerate path to avoid disturbing others without make multiple moving rules, and areas with medium level risk are still passable, when there is no better choice. Besides, the robot will still make the users feel conformable by using effective interactions, like moving slowly to make sure safety or warning the users by sound. The effectiveness of the proposed system is proven by comparing the experimental results with those controlled by conventional potential field method.

INDEX TERMS Autonomous robots; intelligent robots; robot control; social robots

I. INTRODUCTION

Autonomous moving functions that can automatically avoid obstacles and people in the environment while moving to their destinations are important for robots, especially in living spaces of human beings, such as homes and public places [1]. However, most autonomous mobile robots that have been developed so far can recognize surrounding objects and general pedestrians but treat them as obstacles in motion control and perform avoidance behaviors. The considerations for pedestrians in the environment are far from enough [2,3]. For example, robots can ensure the shortest route during path planning, but there are cases where the robot passes through narrow roads or enters into the personal space of pedestrians. The robot is not only more likely to collide with obstacles since it passes through narrow passages, but it can also cause people around them feeling worried or disturbed. Meanwhile, humans usually feel uncomfortable when someone else enters into a certain area around them. This area is called personal space, and a pedestrian's personal space is usually long in the front direction of the person and short in the lateral direction. One's personal space is usually shown as egg shape in horizontal projection. Naturally, this concept of personal space also exists from humans to robots [4], so when a robot enters into this personal space, the person feels discomfort in the same way as when a human enters. For autonomous mobile robots that coexist with humans, it can be said that the behaviors of entering into personal space when moving around should be avoided [5]. In this case, the robot must generate a considerate path that is able to avoid personal spaces and move to the destination naturally.

Meanwhile, when an autonomous mobile robot moves in an environment with multiple people having conversations, the robot should generate a path that takes these cases into consideration. Naturally, passing between two people who are in conversation should be avoided, and it is desirable to control the robot to reach its destination by avoiding entering the spaces among these people. However, if there is no detour route to the destination, the robot should still be able to pass among the people who are in conversation when it is unavoidable. In this case, the robot is better to slow down the moving speed of the robot or a warning sound to remind those people.

Therefore, in this research, an adaptive motion control method for autonomous mobile robots based on integrated potential field method is proposed, which considers the risk map of the environment. Risk map is defined as a map that can show the magnitude of risks in the empty spaces around objects considering the properties of the objects, the concept of which is similar with moving cost in autonomous driving systems [6]. The robot can flexibly generate a considerate moving path that considers the personal spaces of pedestrians and people under conversation and can move autonomously to the destination with the lowest risk. Specifically, the areas where robots

cannot collide with (such as walls and humans) are set in high risk. The areas where it is possible to pass through but are better to be avoided, such as the personal space of humans and spaces among people in conversation, are set as medium or low risk, and the areas suitable for passing through without the above-mentioned obstacles and personal spaces are set as no risk. The robot can flexibly generate a considerate moving path that considers the personal spaces of pedestrians and people under conversation and can move autonomously to the destination with the lowest risk. In this research, global path is planned by using the Dijkstra algorithm based on this risk map. By preferentially selecting the path with lower risk during moving to the destination, a considerate path is generated, considering the properties of people. The robot can also slow down and have a warning sound to interact with the people around when the robot has no choice but to pass through the areas with risks, trying to make the disturbed people feel better.

The contributions of this research are as follows. (1) Defined the concept of risk map, a map to show the magnitude of risks in the empty spaces around objects considering the properties of the objects; (2) Proposed a dynamic path planning method base on risk map. The shorter path with lowest risk is always chosen; (3) Proposed a motion control method based on integrated potential field method. The robot can automatically move with a considerate path to avoid disturbing others without make multiple moving rules, and areas with medium level risk are still passable, when there is no better choice. (4) Effective interactions are designed once someone in the environment is disturbed by the robot. The disturbed people may feel better so that the social acceptance of robots will be improved.

The remainder of this paper is organized as follows. Section II gives a brief review of the related works. Section III shows the design of the proposed mobile robot mechanism. Section IV presents the proposed method of motion control based on risk map and integrated potential field. Section V shows the experiment results. Finally, Section VI concludes the paper.

II. RELATED WROKS

Autonomous mobile robots have gained significant attention in recent years due to their potential applications in factories, offices and homes, etc. These robots, equipped with advanced sensing, perception, and decision-making capabilities, can finish different kinds of tasks and interact with human beings [6-8]. They are applied in numerous fields, including manufacturing [9, 10], logistics [11], healthcare [12], agriculture [13], and search and rescue operations [14, 15]. In manufacturing, they can automate repetitive tasks, improving efficiency and productivity. In logistics, robots can autonomously navigate warehouses and distribution centers, facilitating order fulfillment processes. In healthcare, autonomous mobile robots can assist in patient care, logistics, and disinfection tasks. The agricultural sector benefits from robots performing tasks such as harvesting and crop monitoring, leading to increased productivity. Some service robots have been applied in our daily lives so that people have been familiar with robots [16-18]. However, the social acceptance of mobile robots is still needed to be improved since people are usually interested in robots and cooperate with their tasks, but still feel worried about them so that they usually pay special attention to the robots. One purpose of this paper is to improve the social acceptance of autonomous mobile robots by controlling the robots move considerately.

One of the fundamental aspects of autonomous mobile robots is perception, which involves the ability to sense and interpret the surrounding environment accurately. Sensing technologies such as LiDAR, cameras, and ultrasonic sensors play a crucial role in providing information about the robot's surroundings [19, 20]. Vision-based perception algorithms have been extensively studied, enabling robots to recognize objects, track their movements, and estimate their poses [21]. Additionally, localization and mapping techniques have been developed to enable robots to understand their position within the environment and create detailed maps for navigation purposes [22, 23]. Navigation is a critical capability for autonomous mobile robots as it enables them to move safely and efficiently in complex environments [24]. Path planning algorithms allow robots to determine the optimal paths to their destinations while avoiding obstacles and considering constraints such as energy efficiency [25]. Obstacle avoidance techniques rely on sensor data to detect and circumvent potential obstacles in real-time. Simultaneous Localization and Mapping (SLAM) algorithms have been extensively researched to enable robots to build accurate maps of their surroundings while localizing themselves within those maps [26]. However, the potential occupied spaces of objects are seldom considered. The empty areas around the objects like personal spaces are also needed to be avoided when the robots move around. There are still risks for the robots to pass through these areas since they may disturb others or potentially collide with obstacles that may move suddenly. In this paper, the concept of risk map is defined to evaluate the potential risks of objects.

Efficient control strategies are also essential for autonomous mobile robots to execute their planned trajectories accurately. Various control approaches have been explored, including classical control methods and more advanced techniques such as model predictive control and reinforcement learning [27-30]. These methods aim to optimize the robot's movements, ensuring stability, accuracy, and responsiveness to environmental changes. A novel control method based on integrated potential field considering risk map is proposed in this paper to make the autonomous mobile robot move more considerately. The

control method is effective for most situations without defining kinds of move rules.

As autonomous mobile robots become more and more popular, it is crucial to consider human-robot interaction aspects. Researchers have focused on developing user-friendly interfaces for humans to interact with robots effectively [31-33]. This includes natural language understanding, gesture recognition, and augmented reality interfaces. Understanding and responding to human commands and gestures enable robots to collaborate and assist humans effectively in diverse settings. It is unavoidable to disturb others sometimes when the autonomous mobile robots work around, which is same for the human beings who are working in service industries. Thus, the social robots need to have interaction to make others feel better when they are disturbed. In this paper, some interaction strategies are conducted to make our robot impressive by having good manners.

III. DESIGN OF THE AUTONOMOUS MOBILE ROBOT

Figure 1 shows the overview of the autonomous mobile robot developed in this research. Kobuki developed by YujinRobot is used as the mobile base. Kobuki is an open-source programmable mobile robot developed for research purposes. With two independent driving wheels and two auxiliary wheels, the robot can move forward, reverse and turning around. Depending on the condition of the road surface, the maximum load is 5 [kg] on hard surfaces such as floor, and 4 [kg] on soft surfaces such as carpet. The maximum moving speed is 70 [cm/s] and the maximum turning speed is 180 [deg/s] under unloaded and hard road conditions. A structure consisting of an aluminum frame and two polycarbonate plates are attached on the top of the robot. An RGB-D sensor called Kinect v2, which is developed by Microsoft, is set on the top of the upper plate and a note-book PC is set behind the Kinect sensor for motion control. A LiDAR sensor (URG-04LX-UG01) is set on the lower plate for sensing 2D distance information. In addition, the entire autonomous mobile robot system is composed of another separate PC that performs signal processing such path planning, and these two PCs can communicate by using ROS (Robot Operating System).

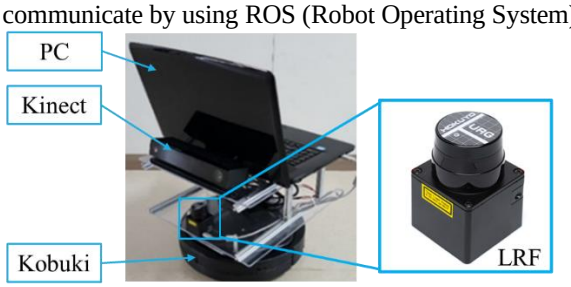

FIGURE 1. **Design of the autonomous mobile robot.**

IV. ROBOT AUTONOMOUS MOTION CONTROL SYSTEM

Figure 2 shows the flowchart of the robot autonomous motion control system developed in this research. The robot autonomously moves to its destination while estimating its self-localization and recognizing people around it based on information gotten from various sensors. Firstly, the sub-PC set on Kobuki is used to recognize the skeleton model of pedestrians based on RGB-D information acquired by Kinect V2 sensor and to send that information to the main PC. Meanwhile, information from the rotary encoders and LiDAR mounted on Kobuki is also sent to the main PC. Based on the LiDAR and rotary encoder information received by the main PC, the self-localization of the robot is estimated while comparing it with the environmental map generated in advance. The legs of pedestrians are detected by using LiDAR information and the skeleton of human beings are detected by using RGB-D information. The detection results are reflected to the risk map. After the destination set by the user manually, the optimal path to the destination is calculated by searching a short path with lowest risk. After that, the motion control commands are sent to the sub-PC mounted on Kobuki to control the robot. Besides, if the generated path still includes the areas of personal spaces or people under conversation, the robot will slow down and emit a warning sound from the sub-PC speaker to remind people around.

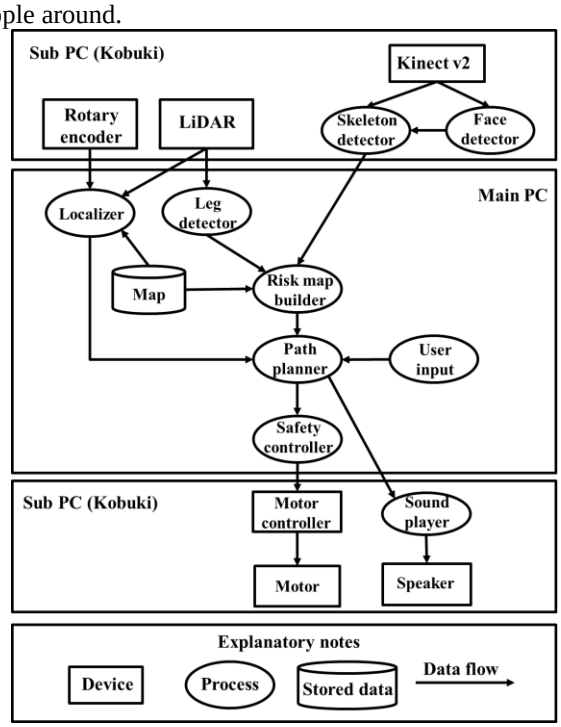

FIGURE 2. **The flowchart of autonomous control system.**

A. ENVIRONMENTAL MAPPING

In order to move autonomously in a specific environment, a map generated in advance is usually needed for the robot. In this study, SLAM (Simultaneous Localization and Mapping) [34] method is used, which generates a map of the environment while achieving self-location at the same time. Especially, the self-localization accuracy is improved by combining the rotary encoders information and the matching result of the point cloud in-formation sent by the LiDAR with

map. The ICP (Iterative Closest Point) algorithm is used for point cloud matching [35]. Fig. 3 (b) shows the map actually generated for the environment shown in Fig. 3 (a). The white areas are shown as empty areas, where the robot can move freely, the black areas are shown as obstacles such as walls, and the gray areas are shown as unknown area. When generating the environmental map in advance, the white areas become wider, the gray areas become smaller, and the black areas appear gradually with the robot moving around. It is observed that the generated map can show the environment well.

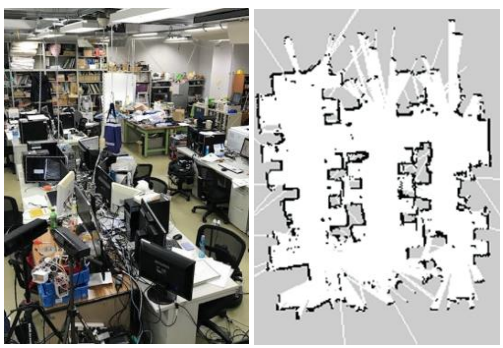

(a) lab environment (b) mapping result by SLAM

FIGURE 3. Mapping result of experimental environment.

B. HUMAN RECOGNITION AND MOVING DIRECTION ESTIMATION

The direction of a person's body is estimated by calculating the normal vector of the vector from the right shoulder to the left shoulder of the skeleton model [36] of the person recognized by Kinect V2, as shown in Equation (1). The position coordinates are calculated in the two-dimensional coordinate system projected onto the ground.

$$\begin{cases} \boldsymbol{R} = \begin{pmatrix} \boldsymbol{cos\,\theta} & \boldsymbol{-sin\,\theta} \\ \boldsymbol{sin\,\theta} & \boldsymbol{cos\,\theta} \end{pmatrix} \\ \boldsymbol{d} = (\boldsymbol{l} - \boldsymbol{r})\boldsymbol{R} \\ \boldsymbol{d}_{normalized} = \dfrac{\boldsymbol{d}}{|\boldsymbol{d}|} \end{cases} \tag{1}$$

Here, $\boldsymbol{l}$ is the position coordinate of the left shoulder, $\boldsymbol{r}$ is the position coordinate of the right shoulder, $\boldsymbol{d}_{normalized}$ is a unit vector representing the direction of the human body, and $\theta = 90\ [deg]$. All position coordinates and vectors are calculated in a two-dimensional coordinate system that is projected onto the ground.

However, the skeleton model recognized by Kinect V2 cannot distinguish the front and back side of the body all the time, with a certain probability of false detection. Thus, front face detection based on harr-like feature is performed and realized by OpenCV [37], and the face detection result is used for correcting the frontal direction of a human body. If a face is recognized at the head position of the skeleton model for a certain period of time, it is determined that the skeleton model is correctly tracked, otherwise it is determined that the front and back are misidentified and tracked.

The robot mainly uses Kinect V2 to recognize the position of a person. Contour detection is also performed to assist human recognition since Kinect V2 has a relatively narrow horizontal viewing angle of 70[deg]. LRF (Laser Rang Finder) is a distance sensor that covers a range of 240[deg] around it. The point cloud gotten by LRF is a set of angles and distance information, and when plotted on a two-dimensional plane, the contours of the surrounding objects appear. Human recognition was extracted by extracting leg candidates by passing LRF information through a classifier whose leg contour information was trained by reinforcement machine learning using Adaptive Boosting (AdaBoost) [38]. A pair of legs that are less than a distance threshold between them is detected as a human and the average coordinates of the two centers of legs are regarded as the position of the person. The information of the person recognized here is processed by a tracking filter based on the Kalman filter to continuously track the person and improve its accuracy. Figure 4 (a) shows a scene with a human being and two chairs, and Fig. 4 (b) shows the detection result by using LRF sensor. The red lines are shown as detected LRF information and the human being, circled by the green line is detected by using the shape information of the two legs. The two chairs are also detected but filtered by the shape information and limitation of distance threshold of two legs.

(a) a person standing in indoor environment

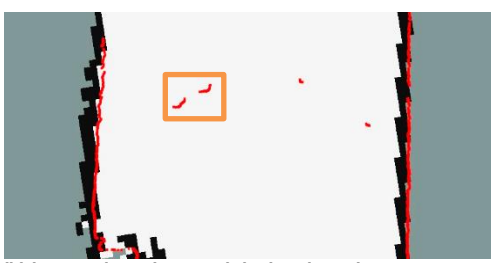

(b) human detection result by leg detection

FIGURE 4. Detection result of a human being by using LEF information.

C. DETECTION OF CONVERSATION STATUS

Detection of conversation status between two persons is achieved by the following rules: the distance between the two should be 2.0[m] or less, and the vector representing the direction of the person body meets the condition of Equation (2).

$$\boldsymbol{d}_1 \cdot \boldsymbol{d}_2 \leq T_i \tag{2}$$

$$|d_1||d_2| \cos\theta_i \leq T_i \quad (3)$$

$$\theta_i \leq \cos^{-1} T_i \quad (4)$$

Here, d_1 is the direction vector of the first person and d_2 is the direction vector of the second person. T_i is the threshold used to judge the state of conversation. Considering the accuracy of estimating the direction of a person, $T_i = -0.8$ is set during the experiment (the angle θ_i formed by the vectors representing the directions of the two persons is 143.13[deg] or more). In addition, Equation (2) can be transformed into Equations (3) and (4). It can also be said that when the angle θ_i between the two directional expressions is 143.13 [deg] or more, it is assumed that they are in a conversational state.

D. RISK MAP OF HUMAN BEINGS AND OBJECTS

Figure 5 (a) and Fig. 5 (b) show the personal space and the area potentially occupied by the persons in conversation. The personal space is long in front of the person, with a length of 117[cm], a maximum width of 80[cm], and a tip width of 32[cm]. The area potentially occupied by two persons in conversation has a shape in which the personal spaces of each person are connected face to face, and the maximum distance between the two is set as 200[cm]. The potential occupied spaces generated by the people in Fig. 5 (a) and Fig. 5 (b), which are reflected to the space risk map, are shown in Fig. 5 (c) and Fig. 5 (d) separately. Notice that the range shown in light blue is a high-risk area where people exist and is judged to be impassable since it may cause collision after considering the radius of the robot. High risk regions are represented as red color, and moderate-risk and low-risk regions are shown with colors changing from red to purple. No-risk areas are represented as gray color. The level of risk is proportional to the distances to the center places of human beings.

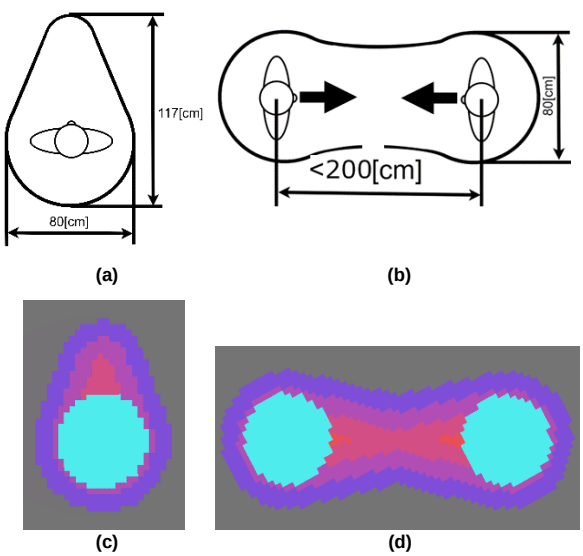

FIGURE 5. Risk map generated by a human being: (a) personal space; (b) occupied space by 2 people under conversation; (c) potentially occupied space of a human being; (d) potentially occupied space by 2 people under conversation.

Similarly, the risk map of the scene in Fig. 3 is shown in Fig. 6. Same risk levels are set to different objects, since all kinds of objects are treated as obstacles here. The robot needs to avoid colliding with the objects, considering an allowance error distance between the robot and obstacles, which makes sure the robot keeps a distance with obstacles. The potential occupied space ranges of objects are smaller than that of human beings since the objects have no emotions and the robot can get closer to them than human being, who have the concept of personal spaces.

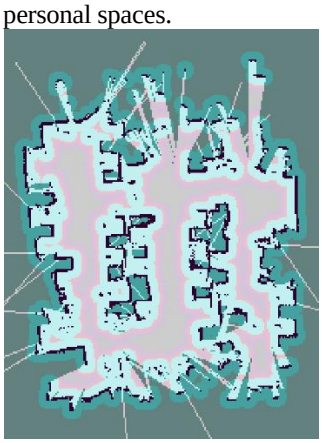

FIGURE 6. Risk map generated from mapping result.

E. ADAPTIVE MOTION CONTROL

The global path is calculated using the Dijkstra method [39], which considers the risk map. Here, the risk map is defined as a map that indicates the degree of risk of an area in stages. High risks are set in areas where collisions are not allowed, such as walls, obstacles and people. Potentially occupied area is set with moderate risk. Empty space is set with no risk. The Dijkstra algorithm is able to calculate the shortest path between two nodes on a graph composed of nodes and edges. The cost is calculated according to the risk information of the risk map for the nodes placed in the space where the robot can move, and the path that minimizes the sum of the costs is calculated. In this way, the nodes with lower risk are chosen to form the path. Instead of calculating a shortest path, a comparatively short path with lowest risk is generated. Generally, the robot chooses the path with no risk. Potential occupied places with moderate risk can still be chosen when there is no path that can be generated with no risk.

In addition, when the robot cannot avoid entering a medium-risk area such as the personal space area, the robot slows down and emits a warning sound to remind the people around, making them feel better with these interactions like human beings.

Figure 7 (a) shows the path planning result by using the Dijkstra method without using the risk map, and Fig. 7(b) shows path planning result based on the risk map. In the figure, green curves represent paths, gray areas represent areas that are able to move around, and black areas represent obstacles. It is observed that a better and more nature path of passing through wide way in the middle of obstacles with lowest risk

This article has been accepted for publication in IEEE Access. This is the author's version which has not been fully edited and content may change prior to final publication. Citation information: DOI 10.1109/ACCESS.2023.3292999

is generated when using the risk map since the narrow way (shown in Fig. 7 (a)) passes through the potentially occupied areas of objects.

The motion of the robot is controlled by potential field method [40]. Attractive potential filed is generated from sub-goals on the path. When the goal for the robot is set and moving path is generated, sub-goals are generated by sampling from the path in equal interval, which can improve the situation that the robot stops at local extremums. The attractive force F_{ag} from the subgoal is set as Equation (5).

$$F_{ag} = k_{ag} \times d_g \tag{5}$$

Here, k_{ag} is the attraction coefficient for the goal, and d_g is the distance from the subgoal to the robot. The attractive potential P_{ag} generated is given by Equation (6).

$$P_{ag} = \frac{k_{ag}}{2} \times {d_g}^2 \tag{6}$$

The repulsive potential is normally generated from obstacles. The repulsive force F_{ro} from each point of the objects is set as Equation (7).

$$F_{ro} = \frac{k_{ro}}{(d_{ro}-d_0)^2}, if\ d_{ro} > d_0 ; F_{ro} = \infty, else \tag{7}$$

Here k_{ro} is the repulsion coefficient for the objects, d_{ro} is the distance from the object to the robot, and d_0 is the minimum distance to be allowed by the robot to reach the object. The repulsive potential P_{ro} generated is given by Equation (8).

$$P_{ro} = \frac{k_{ro}}{d_{ro}-d_0}, if\ d_{ro} > d_0 ; P_{ro} = \infty, else \tag{8}$$

The repulsive potential fields are also set in the places where risks are generated based on the risk map. The repulsive force F_{rp} from each potential occupied area of the objects is set as Equation (9).

$$F_{rp} = \frac{k_{rp}}{(d_{rp}-d_0)^2}, if\ d_{max} > d_{rp} > d_0 ; F_{rp} = 0, else \tag{9}$$

The repulsive potential P_{rp} generated is given by Equation (10).

$$P_{rp} = \frac{k_{rp}}{d_{rp}-d_0}, if\ d_{max} > d_{rp} > d_0 ; P_{rp} = 0, else \tag{10}$$

Here, k_{rp} is the repulsion coefficient for the potential field areas and is different for different kinds of objects. It is a constant value for normal objects with potential occupied spaces, and a variable value for objects with directions (like egg shape for personal space). The values of k_{rp} are defined in advance. d_{rp} is the distance from the object to the robot, and d_{max} is the maximum distance of potential occupied area.

The integrated potential field will be generated, and the robot will move towards the gradient direction of integrated potential field.

Figure 8 shows the integrated potential field status during moving to the destination. The robot moved from the bottom (shown as Fig. 8 (a)) to the top (shown in Fig. 8 (i)) in the map. Figure 9 shows the integrated potential field status around the robot when 2 independent people were standing in the environment.

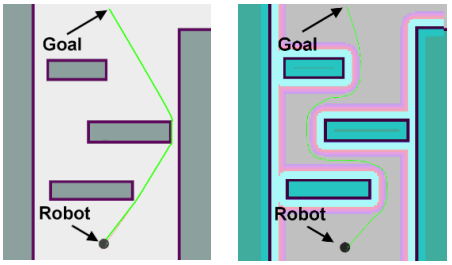

FIGURE 7. Risk map generated from mapping result.

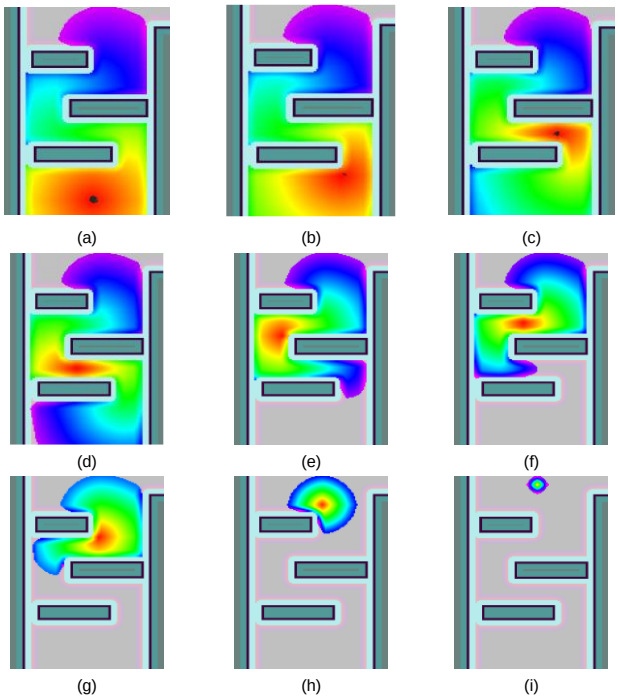

FIGURE 8. Moving towards destination based on space risk map: (a)~(i) integrated potential field status during moving to the destination.

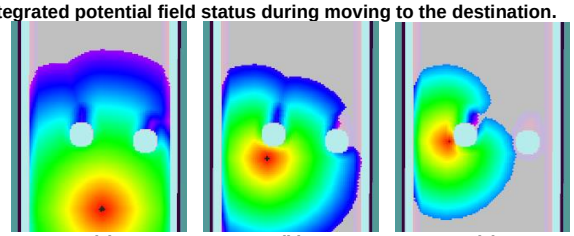

FIGURE 9. Integrated potential field status during moving around 2 people to the destination.

V. EXPERIMENTAL RESULTS

To evaluate the effectiveness of the proposed method, experiments that estimating the facing directions of human beings and making the robot move under different kinds of environments automatically are conducted. Different kinds of objects and people under different status appeared in the environment and the robot shows different performances by using traditional method of potential field method and the proposed method of considering space risk map.

A. Experiments of Human Facing Direction Estimation

To confirm the accuracy of facing direction estimation of a person recognized by Kinect V2, a person turns around in front of the robot. It is confirmed that the skeleton model can recognize the persons normally and estimate the direction of the person for most time (shown in Fig.10 (a)), but sometimes the direction of front or back can be misidentified (shown in Fig.10 (b) and Fig.10 (c)). Moreover, the misidentification can be corrected by fusing face recognition result that detected by using OpenCV. The detection results are shown in Fig. 11. The direction of the person in experiment can always be recognized correctly and the potential occupied space are also generated as well as that of the walls in the environment.

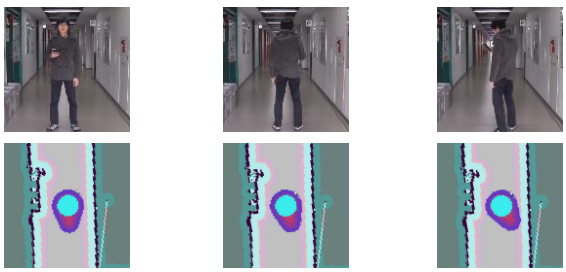

FIGURE 10. **Human detection and facing direction estimation result by using skeleton model: (a)correct estimation result; (b) misidentification result of facing behind; (c) misidentification result of facing aside.**

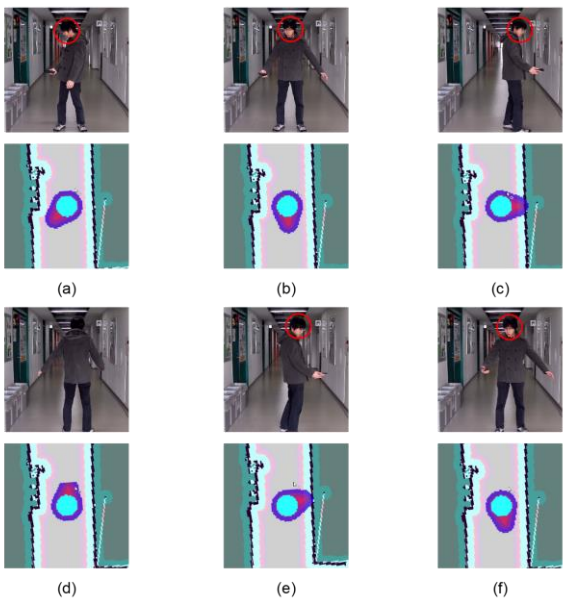

FIGURE 11. **Human detection and facing direction estimation result by using proposed method of fusing face detection result: (a)~(f) correct facing direction estimation results in different poses.**

B. Dynamic Path Planning Considering Personal Space

Figure 11 shows how the robot avoids the personal space of a person in the center of the passage. Since the person is facing left as shown in Fig. 12 (a), a risk map reflecting personal space is generated, and the robot shown in Fig. 12 (a)~(d) moves behind the person to get to its destination since the spaces in front of the person are all with moderate risk. To compare the result with the conventional method based on potential field method without considering the risk map, Fig. 16 (a) shows the shortest path under the same condition. The robot moves in front of the person and disturbs the person. Figure 13 shows how the robot avoids the personal space of a person in the left side of the passage. The person is facing right as shown in Fig. 13 (a), a risk map reflecting personal space is generated, and the robot shown in Fig. 13 (a)~(d) moves in front the person to get to its destination since the spaces behind the person have higher risk.

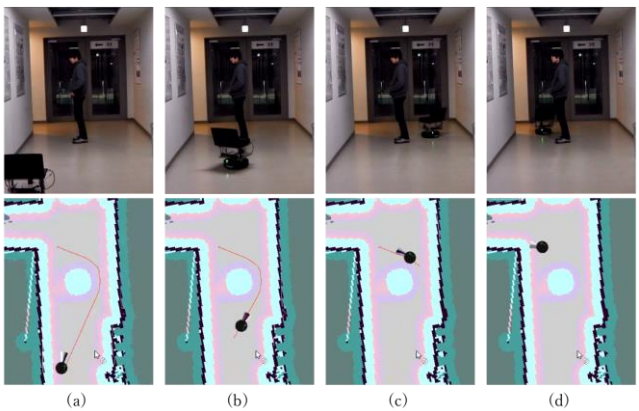

FIGURE 12. **Robot motions when avoiding personal space by going behind of the person: (a)~(d) Moving path considering risk map.**

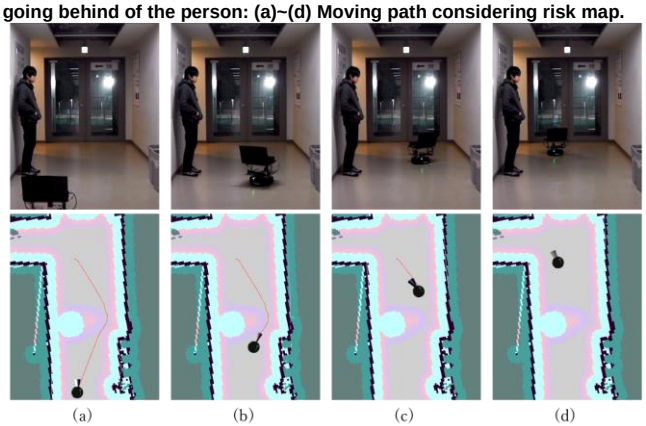

FIGURE 13. **Robot motions when avoiding personal space by going in front of the person: (a)~(d) Moving path considering risk map.**

Figure 14 shows how the robot gets through the personal space of a person near the center of the passage. Since the person is facing right as shown in Fig. 14 (a), a risk map reflecting personal space is generated, and the robot shown in Fig. 14 (a)~(d) moves in front of the person to get to its destination since the spaces behind the person have higher risk. The robot moves to the destination by choosing the path with lowest risk, but it still entered personal space area of the person. It was also observed that the robot decelerates and emits a warning sound immediately before entering the personal space to make him feel better. To compare the result with the conventional method based on potential field method without considering the risk map, Fig. 16 (b) shows the shortest path under the same conditions. The robot moves in front of the person but gets too close to the person without any interactions, which leads to the person feeling more uncomfortable.

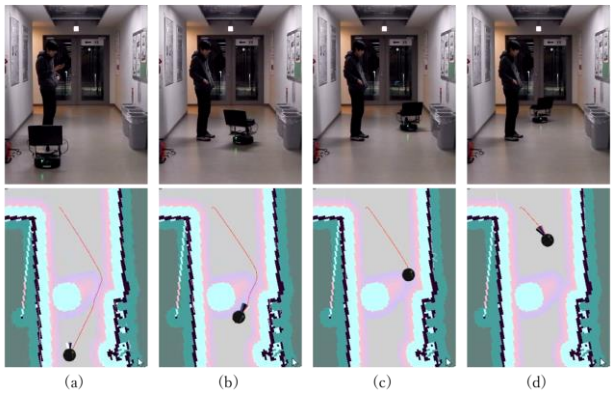

FIGURE 14. **Robot motions when getting through personal space unavoidability by going in front of the person: (a)~(d) Moving path considering risk map.**

Figure 15 shows the autonomous moving result of the robot considering the personal space of multiple people who are not in conversation in a crowded situation. The robot generated a risk map based on the directions of multiple personal spaces and generated a path with lowest risk, as shown in Fig. 15 (a)~(d). The robot moves through the right two people and keeps a certain distance with these two people. It was also observed that the robot decelerates and emits a warning sound immediately before entering their personal space to make them feel better. To compare the result with the conventional method based on potential field method without considering the risk map, Fig. 16 (c) shows the shortest path under the same conditions. The robot also moves through the right two people but gets very close to one person, which make the person feel more uncomfortable.

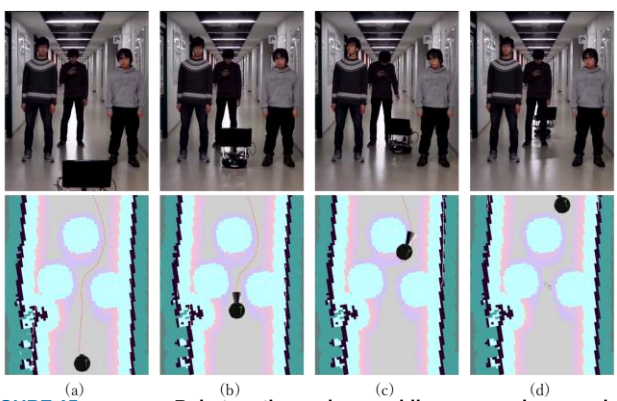

FIGURE 15. **Robot motions when avoiding personal spaces by going through the persons: (a)~(d) Moving path considering risk map.**

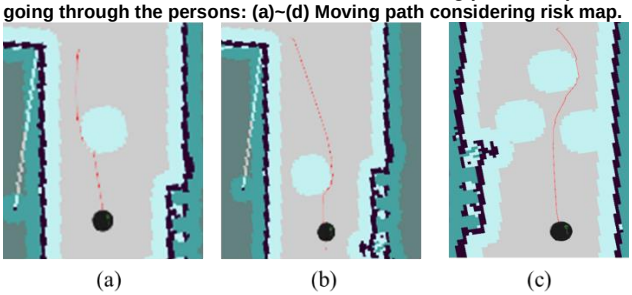

FIGURE 16. **Robot motions when avoiding persons in shortest paths: (a)~(c) Moving path without considering risk map.**

C. Dynamic Path Planning Considering Space Risk Map of Multiple People in Conversation

Figure 17 shows how the robot avoids moving among people in conversation. There are two people facing each other on the right side of the corridor shown in Fig. 17 (a). The risk map was generated, and the destination was reached by avoiding the area with risk between the two people, as shown in Fig. 17 (a)~(d). To compare the result with the conventional method based on potential field method without considering the risk map, Fig. 19 (a) shows the shortest path under the same conditions. The robot moves between the two people in conversation and disturbs them without any interactions, which makes the people feeling uncomfortable.

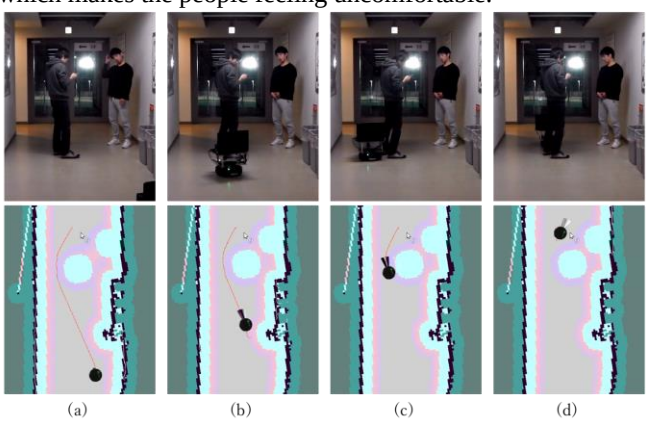

FIGURE 17. **Robot motions when avoiding two persons in conversation by going behind: (a)~(d) Moving path considering risk map.**

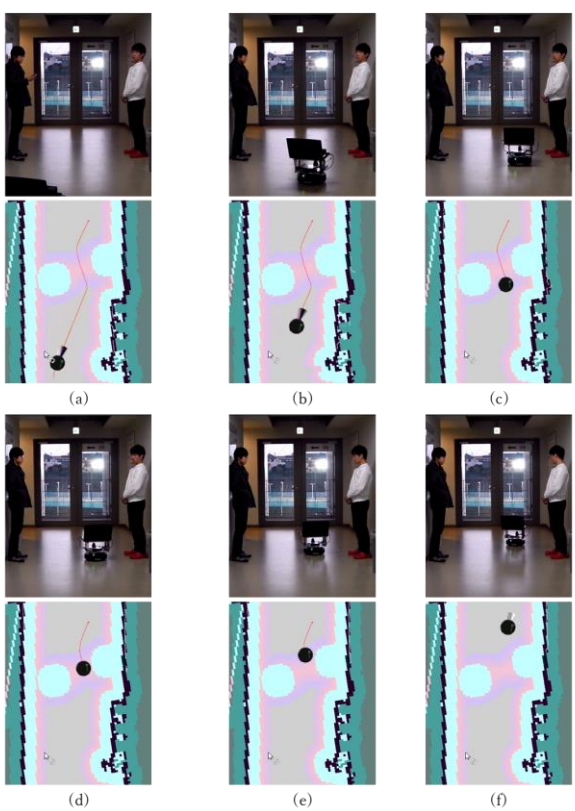

FIGURE 18. **Robot motions when avoiding two persons in conversation by go through of them unavoidably: (a)~(d) Moving path considering risk map.**

Figure 18 shows how the robot unavoidably moves between two people in conversation. There are two people on both sides of the passage shown in Fig. 18 (a), and the two face each other in conversation. Since it does not exist a path without risk, the robot shown in Fig. 18 (a)~(d) got to its destination by passing exactly halfway between the two with the lowest risk path. It was also observed that the robot decelerates and emits a warning sound just before it enters the area between the two people to make them feel better. To compare the result with the conventional method based on potential field method without considering the risk map, Fig. 19 (b) shows the shortest path under the same conditions. It disturbs them without any reactions and gets too close to one person, which makes them feel uncomfortable.

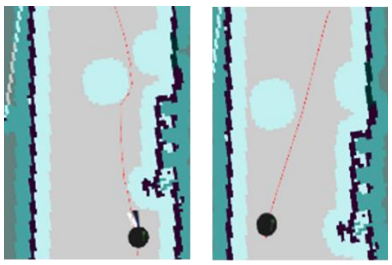

FIGURE 19. Robot motions when avoiding persons under conversations in shortest paths: (a)~(b) Moving path without considering risk map.

VI. CONCLUSION

In this research, by defining the concept of risk map and applying it into the process of motion control of the robot, a path with lowest risk is generated, which enables the robot considering the personal spaces and situations of human beings who are in conversations. The robot can move to the destination considerately and naturally, trying its best to not to disturb other people or make them feel uncomfortable. In case that it is unavoidable to enter the personal spaces or disturb people for finishing its task, the robot still can make them feel better through effective interactions like slowing down and warning them by sound. Experimental results have shown that the generated paths are more considerate to the people in the environment. In the future, the risk map is needed to be improved by setting different values for different objects. Potential occupied space and risk level of an object reflected in the risk map should be adjusted appropriately according to the object's types, velocity and acceleration.

REFERENCES

[1] C. -S. Chen and S. -Y. Lin, "Costmap Generation Based on Dynamic Obstacle Detection and Velocity Obstacle Estimation for Autonomous Mobile Robot," 2021 21st International Conference on Control, Automation and Systems (ICCAS), Jeju, Korea, Republic of, 2021, pp. 1963-1968, doi: 10.23919/ICCAS52745.2021.9649733.

[2] F. Cherni, Y. Boutereaa, C. Rekik and N. Derbel, "Autonomous mobile robot navigation algorithm for planning collision-free path designed in dynamic environments," 2015 9th Jordanian International Electrical and Electronics Engineering Conference (JIEEEC), Amman, Jordan, 2015, pp. 1-6, doi: 10.1109/JIEEEC.2015.7470747.

[3] Kazushi Nakazawa, Keita Takahashi, Masahide Kaneko, "Movement Control of Accompanying Robot Based on Artificial Potential Field Adapted to Dynamic Environments," *Electrical Engineering in Japan,* Volume 192, No. 1, 2015, pp. 25-35.

[4] M. Lauckner, F. Kobiela and D. Manzey, "'Hey robot, please step back!' - exploration of a spatial threshold of comfort for human-mechanoid spatial interaction in a hallway scenario," The 23rd IEEE International Symposium on Robot and Human Interactive Communication, Edinburgh, UK, 2014, pp. 780-787, doi: 10.1109/ROMAN.2014.6926348.

[5] B. Tribelhorn and Z. Dodds, "Evaluating the Roomba: A low-cost, ubiquitous platform for robotics research and education," Proceedings 2007 IEEE International Conference on Robotics and Automation, Rome, Italy, 2007, pp. 1393-1399, doi: 10.1109/ROBOT.2007.363179.

[6] D. Reichardt and J. Shick, "Collision avoidance in dynamic environments applied to autonomous vehicle guidance on the motorway," Proceedings of the Intelligent Vehicles '94 Symposium, Paris, France, 1994, pp. 74-78, doi: 10.1109/IVS.1994.639475.

[7] M. -G. Kim, H. Yoon, J. Kim, J. Kim, D. -S. Sohn and K. Kim, "Investigating Frontline Service Employees to Identify Behavioral Goals of Restaurant Service Robot: An Exploratory Study," 2021 18th International Conference on Ubiquitous Robots (UR), Gangneung, Korea (South), 2021, pp. 57-62, doi: 10.1109/UR52253.2021.9494675.

[8] D. Sanjay, M. C. Chinnaiah, T. S. Savithri and P. R. Kumar, "A survey of reconfigurable service robots," 2016 International Conference on Research Advances in Integrated Navigation Systems (RAINS), Bangalore, India, 2016, pp. 1-4, doi: 10.1109/RAINS.2016.7764426.

[9] K. Daeinabi and M. Teshnehlab, "Industrial Arc Welding Robot Defect Tracking System in Automotive Industry," 2007 International Conference on Mechatronics and Automation, Harbin, China, 2007, pp. 3937-3941, doi: 10.1109/ICMA.2007.4304204.

[10] M. Nam, S. Mun, J. Lee and J. Lee, "The angle cutting robot system in the shipbuilding industry," 2015 IEEE International Conference on Advanced Intelligent Mechatronics (AIM), Busan, Korea (South), 2015, pp. 1463-1466, doi: 10.1109/AIM.2015.7222747.

[11] P. Detzner, T. Kirks and J. Jost, "A Novel Task Language for Natural Interaction in Human-Robot Systems for Warehouse Logistics," 2019 14th International Conference on Computer Science & Education (ICCSE), Toronto, ON, Canada, 2019, pp. 725-730, doi: 10.1109/ICCSE.2019.8845336.

[12] J. Han, H. -J. Kang and G. H. Kwon, "Understanding the servicescape of nurse assistive robot: The perspective of healthcare service experience," 2017 14th International Conference on Ubiquitous Robots and Ambient Intelligence (URAI), Jeju, Korea (South), 2017, pp. 644-649, doi: 10.1109/URAI.2017.7992693.

[13] X. -k. Xu, X. -m. Li and R. -h. Zhang, "Remote Configurable Image Acquisition Lifting Robot for Smart Agriculture," 2019 IEEE 4th Advanced Information Technology, Electronic and Automation Control Conference (IAEAC), Chengdu, China, 2019, pp. 1545-1548, doi: 10.1109/IAEAC47372.2019.8997721.

[14] Z. Xuexi, A. Yuming, F. Genping, L. Guokun and L. Shiliu, "Survey on Key Technology of Robocup Rescue Robot," 2019 Chinese Control Conference (CCC), Guangzhou, China, 2019, pp. 4746-4750, doi: 10.23919/ChiCC.2019.8866137.

[15] L. Zhu, G. Liu, Y. Zhao, C. Liu, M. Jiang and X. Li, "Design of Motion Control System of Rescue Robot Based on ARM," 2017 International Conference on Computer Technology, Electronics and Communication (ICCTEC), Dalian, China, 2017, pp. 1183-1186, doi: 10.1109/ICCTEC.2017.00257.

[16] B. G. Draghici, A. E. Dobre, M. Misaros and O. P. Stan, "Development of a Human Service Robot Application Using Pepper Robot as a Museum Guide," 2022 IEEE International Conference on Automation, Quality and Testing, Robotics (AQTR), Cluj-Napoca, Romania, 2022, pp. 1-5, doi: 10.1109/AQTR55203.2022.9802037.

[17] H. S. Al-Khalifa, B. Alsalman, D. Alnuhait, A. Alkhalifah, O. Meldah and S. Aloud, "The experience of developing Mr. saud educational system using NAO humanoid robot," 2017 6th International Conference on Information and Communication Technology and

Accessibility (ICTA), Muscat, Oman, 2017, pp. 1-3, doi: 10.1109/ICTA.2017.8336008.

[18] R. Aminuddin, A. Sharkey and L. Levita, "Interaction with the Paro robot may reduce psychophysiological stress responses," 2016 11th ACM/IEEE International Conference on Human-Robot Interaction (HRI), Christchurch, New Zealand, 2016, pp. 593-594, doi: 10.1109/HRI.2016.7451872.

[19] F. Yang, W. Liu, W. Li, L. Fang, D. Sun and H. Yuan, "A Novel Object Detection and Localization Approach via Combining Vision with Lidar Sensor," 2021 IEEE 4th International Conference on Electronics Technology (ICET), Chengdu, China, 2021, pp. 167-172, doi: 10.1109/ICET51757.2021.9451151.

[20] S. Shoval and J. Borenstein, "Using coded signals to benefit from ultrasonic sensor crosstalk in mobile robot obstacle avoidance," Proceedings 2001 ICRA. IEEE International Conference on Robotics and Automation (Cat. No.01CH37164), Seoul, Korea (South), 2001, pp. 2879-2884 vol.3, doi: 10.1109/ROBOT.2001.933058.

[21] M. G. Krishnan and A. S, "Object detection methods for Image-based Visual Servoing of 6-DOF Industrial robot," 2022 IEEE Region 10 Symposium (TENSYMP), Mumbai, India, 2022, pp. 1-6, doi: 10.1109/TENSYMP54529.2022.9864432.

[22] L. Qu and H. Wang, "An overview of Robot SLAM problem," 2011 International Conference on Consumer Electronics, Communications and Networks (CECNet), Xianning, China, 2011, pp. 1953-1956, doi: 10.1109/CECNET.2011.5769022.

[23] Z. -X. Li, G. -H. Cui, C. -L. Li and Z. -S. Zhang, "Comparative Study of Slam Algorithms for Mobile Robots in Complex Environment," 2021 6th International Conference on Control, Robotics and Cybernetics (CRC), Shanghai, China, 2021, pp. 74-79, doi: 10.1109/CRC52766.2021.9620122.

[24] Lixin Tang and S. Yuta, "Vision based navigation for mobile robots in indoor environment by teaching and playing-back scheme," Proceedings 2001 ICRA. IEEE International Conference on Robotics and Automation (Cat. No.01CH37164), Seoul, South Korea, 2001, pp. 3072-3077 vol.3, doi: 10.1109/ROBOT.2001.933089.

[25] Lixin Tang and S. Yuta, "Indoor navigation for mobile robots using memorized omni-directional images and robot's motion," IEEE/RSJ International Conference on Intelligent Robots and Systems, Lausanne, Switzerland, 2002, pp. 269-274 vol.1, doi: 10.1109/IRDS.2002.1041400.

[26] D. -T. Ngo and H. -A. Pham, "Towards a Framework for SLAM Performance Investigation on Mobile Robots," 2020 International Conference on Information and Communication Technology Convergence (ICTC), Jeju, Korea (South), 2020, pp. 110-115, doi: 10.1109/ICTC49870.2020.9289428.

[27] K. Zhu and T. Zhang, "Deep reinforcement learning based mobile robot navigation: A review," in Tsinghua Science and Technology, vol. 26, no. 5, pp. 674-691, Oct. 2021, doi: 10.26599/TST.2021.9010012.

[28] Y. Yi, F. Mengyin, S. Changsheng, W. Meiling and Z. Cheng, "Control Law Design of Mobile Robot Trajectory Tracking and Development of Simulation Platform," 2007 Chinese Control Conference, Zhangjiajie, China, 2007, pp. 198-202, doi: 10.1109/CHICC.2006.4347355.

[29] Do-Young Yoon, Sang-Rok Oh, Gwi-Tae Park and Bum-Jae You, "A biologically inspired homeostatic motion controller for autonomous mobile robots," 2003 IEEE International Conference on Robotics and Automation (Cat. No.03CH37422), Taipei, Taiwan, 2003, pp. 3158-3163 vol.3, doi: 10.1109/ROBOT.2003.1242076.

[30] C. Tarin, H. Brugger, E. P. Hofer and B. Tibken, "Combining trajectory control and position control for autonomous mobile robot navigation," 2001 European Control Conference (ECC), Porto, Portugal, 2001, pp. 1804-1809, doi: 10.23919/ECC.2001.7076183.

[31] U. Nagarajan, G. Kantor and R. L. Hollis, "Human-Robot Physical Interaction with dynamically stable mobile robots," 2009 4th ACM/IEEE International Conference on Human-Robot Interaction (HRI), La Jolla, CA, USA, 2009, pp. 281-282.

[32] Y. Kobayashi et al., "Assisted-care robot dealing with multiple requests in multi-party settings," 2011 6th ACM/IEEE International Conference on Human-Robot Interaction (HRI), Lausanne, Switzerland, 2011, pp. 167-168, doi: 10.1145/1957656.1957714.

[33] D. Das, M. G. Rashed, Y. Kobayashi and Y. Kuno, "Recognizing Gaze Pattern for Human Robot Interaction," 2014 9th ACM/IEEE International Conference on Human-Robot Interaction (HRI), Bielefeld, Germany, 2014, pp. 142-143.

[34] Bin Zhang, Masahide Kaneko and Hun-ok Lim, "2D Mapping Integrating with 3D information for the Autonomous Mobile Robot under Dynamic Environment," Electronics, Volume 8, No. 12, 2019, pp. 1-11.

[35] S. Rusinkiewicz and M. Levoy, "Efficient variants of the ICP algorithm," Proceedings Third International Conference on 3-D Digital Imaging and Modeling, Quebec City, QC, Canada, 2001, pp. 145-152, doi: 10.1109/IM.2001.924423.

[36] J. Shotton et al., "Real-time human pose recognition in parts from single depth images," CVPR 2011, Colorado Springs, CO, USA, 2011, pp. 1297-1304, doi: 10.1109/CVPR.2011.5995316.

[37] P. Viola and M. Jones, "Robust real-time face detection," Proceedings Eighth IEEE International Conference on Computer Vision. ICCV 2001, Vancouver, BC, Canada, 2001, pp. 747-747, doi: 10.1109/ICCV.2001.937709.

[38] Yoav Freund, Robert E Schapire, " A Decision-Theoretic Generalization of On-Line Learning and an Application to Boosting," Journal of Computer and System Sciences, Volume 55, Issue. 1, 1997, pp. 119-139.

[39] A. Alyasin, E. I. Abbas and S. D. Hasan, "An Efficient Optimal Path Finding for Mobile Robot Based on Dijkstra Method," 2019 4th Scientific International Conference Najaf (SICN), Al-Najef, Iraq, 2019, pp. 11-14, doi: 10.1109/SICN47020.2019.9019345.

[40] Bin Zhang, Tomoaki Nakamura and Masahide Kaneko, " A Framework for Adaptive Motion Control of Autonomous Sociable Guide Robot," IEEJ Transactions on Electrical and Electronic Engineering, Volume 11, Issue. 6, 2016, pp. 786-795.

Bin Zhang graduated in 2011 graduated from Harbin Engineering University (Dept. of Automation), in 2017 completed doctorate at University of Electro-Communications (Grad. School of Informatics and Eng.). D. Eng. Now he is an assistant professor at Kanagawa University (Fac. of Eng., Dept. of Mech. Eng.). He is researching in intelligent robotics, signal processing, artificial intelligence, human interaction and other fields. Membership: RSJ, JSME, IEEJ, IEEE.

Ryuji Sengoku is researching on robotics. He received his B.E. degree in 2020 in department of Mechanical Engineering from Kanagawa University, Japan.

Hun-ok Lim is a vice president of Kanagawa University. He received a B.E. degree in Electrical Engineering from Hongik University, South Korea, and an M.E. and Ph.D. in Mechanical Engineering from Waseda University, Japan. From 2000 to 2005, he was an associate professor in the Department of System Design Engineering, Kanagawa Institute of Technology. In 2005, he joined the Department of Mechanical Engineering at Kanagawa University. Since then, he has held several positions at the university, including dean of the Faculty of Engineering (2014-2020), a trustee on the Board of Trustees (2017-2020), dean of the Graduate School of Engineering (2020-2022), and director of the Center for Cooperation with Society since 2022. Since 2000, he has been with the Humanoid Robotics Institute, Waseda University, where he is currently a visiting professor. He was also a visiting research scientist at the Department of Mechanical and Industrial Engineering at the University of Toronto, Canada, from 2009 to 2010. His research interests include humanoid robots, walking systems, human-robot symbiosis systems, human-centered robotics, human safety control, emotion-based control, compliance control, and mobile manipulator control. He is a senior member of the IEEE, a member of the Robotics Society of Japan, and a member of the Japanese Society of Instrument and Control Engineers. Since 2010, he is an Associate Editor of International Journal of Humanoid Robotics.